Interface relaxation and electronic corrugation in the Pb/Si(111)-Pb-α-$\sqrt{3}\times\sqrt{3}$

M. Hupalo, V. Yeh, T. L. Chan, C. Z. Wang, K. M. Ho, and M. C. Tringides*
Department of Physics, Iowa State University and Ames Laboratory—U.S. DOE, Ames, Iowa 50011, USA
(Received 10 August 2004; revised manuscript received 22 October 2004; published 31 May 2005)

The corrugation observed on top of Pb islands grown on Si(111)-Pb-α-$\sqrt{3}\times\sqrt{3}$ (as a result of the Moire pattern formation at the Si/Pb interface) offers a different way to obtain information about the interface. Results from several probes (high resolution LEED, STM, STS, model image calculations) are compared. The origin of the corrugation is predominantly geometric (because of layer relaxation in the island) and to a lesser degree electronic (related to the confined electrons within the island). This is deduced from the hexagonal ringlike features in LEED and the quantitative comparison of the corrugation contrast in calculated vs measured STM and STS images.

DOI: 10.1103/PhysRevB.71.193408 PACS number(s): 68.55.Jk, 68.65.Fg

The confinement of electrons in low dimensional structures results in sharp quantization of their energy levels which is commonly referred to as quantum size effects (QSE).[1,2] The energy level position depends sensitively on the dimensions of the grown structures and one of the goals is to search with spectroscopic techniques [i.e., angle resolved photoemission and scanning tunneling spectroscopy (STS)] for evidence of QSE in epitaxially grown structures.[3,4] It was found that QSE are not only observable spectroscopically, but more importantly they modify the energy stability of a grown island with its height, so a very sharp distribution of preferred heights has been seen.[5] This offers different pathways to self-organization on the nanoscale. Preferred heights have been observed also in the growth of Ag/GaAs(110),[6] and been accounted for in terms of the competition between confinement and charge transfer.[7] Such models have been partially justified from first principles calculations on free standing Pb films[8] or in mixed models with the overlayer treated as stabilized jellium and the substrate as 1D pseudopotentials.[9]

Experiments of Pb deposition on different interfaces at low temperatures have shown that uniform height islands can be grown with preferred height which depends on the initial interface, i.e., 7-step islands on Si(111)-7×7 and 5-step islands on the Si(111)-Pb($\sqrt{3}\times\sqrt{3}$).[10] Not many experimental techniques are available to probe buried interfaces. In this work we show how the corrugation observed on top of Pb islands grown on Si(111)-Pb-α($\sqrt{3}\times\sqrt{3}$) (which originates from the Moire pattern of overlaying the Pb(111) and Si(111) lattices) can be used to deduce information about the interface. As demonstrated earlier[4,11] the corrugation depends on the tunneling voltage, so its origin must be partially due to electronic effects, i.e., the projection to the top of the relative phase $\phi(x,y)$ of the confined electron wave function at the buried interface. However there can be an additional purely geometric contribution to the corrugation, which is related to the relaxation of the Pb layers.[12]

For growth on Si(111)-(7×7) the corrugation has the 7×7 periodicity and the 7×7 reconstruction is still intact underneath the islands,[4,13] but for growth on top of the α-$\sqrt{3}\times\sqrt{3}$ the corrugation is related to the "beating" period between the (1×1) Si and (1×1) Pb lattices. The most often observed period is $\lambda=3.5$ nm which is the matching distance of 9 Si with 10 Pb(111) lattice constants. As discussed in Ref. 14 other less frequent orientations between the two "beating" lattices are possible. X-reflectivity experiments show that underneath the islands the $\sqrt{3}\times\sqrt{3}$ reconstruction is removed and Si(1×1) is in contact with Pb(111) islands.[13]

The corrugation is observed with high resolution LEED from a ringlike intensity distribution. This confirms the strong contribution of the geometric relaxation, since the LEED intensity distribution vs scattering wave vector originates from variation in atom position normal to the surface. LEED probes easier larger wave vectors (and therefore smaller distances in real space) so it provides the shape of the "overlapping" regions in the Moire pattern. In a different use of diffraction[15] the dependence of reflectivity on incident beam energy was used to map out the electronic band structure of an epitaxially grown film but no structural information was deduced about the buried interface as in the current work.

On the other hand an electronic effect originates from the confined electrons within the islands and no variation in atom position normal to the surface is necessary. The confined electrons are described with subbands of constant wave vector k_z (normal to the surface) and with parallel component $k_\parallel$ in the range $(0<k^\parallel<((2mE_f/h^2)\text{-}k_z^2)^{1/2})$, where E_f is the Fermi energy.[4,16] The "beating" periodicity λ between the two lattices defines the wave vector $q\approx2\pi/\lambda$ which is best observed at $k^\parallel\sim q$.[17] Since the energy corresponding to the corrugation wave vector $E_\parallel=(\hbar q)^2/2m$ is only 0.1 eV (for $\lambda\approx3.5$ nm), this implies that $k^\parallel\sim q$ is met at energies just above the discrete energy levels E_z. This implies that the signature of the electronic effect is the dependence of the corrugation amplitude on tunneling voltage and island height. It was suggested that in addition to these two factors, the stacking sequence in the fcc(111) Pb island, whether ABC or ACB, can introduce a lateral phase shift in the confined electron wave function.[11] The conditions necessary for the corrugation contrast to change (i.e., whether the compact regions or the complementary interconnected "sea" between them is bright or not) have been discussed in Ref. 12.

Figures 1(a) and 1(b) show a high resolution LEED pattern close to the specular (00) and Si(10) spots after depos-

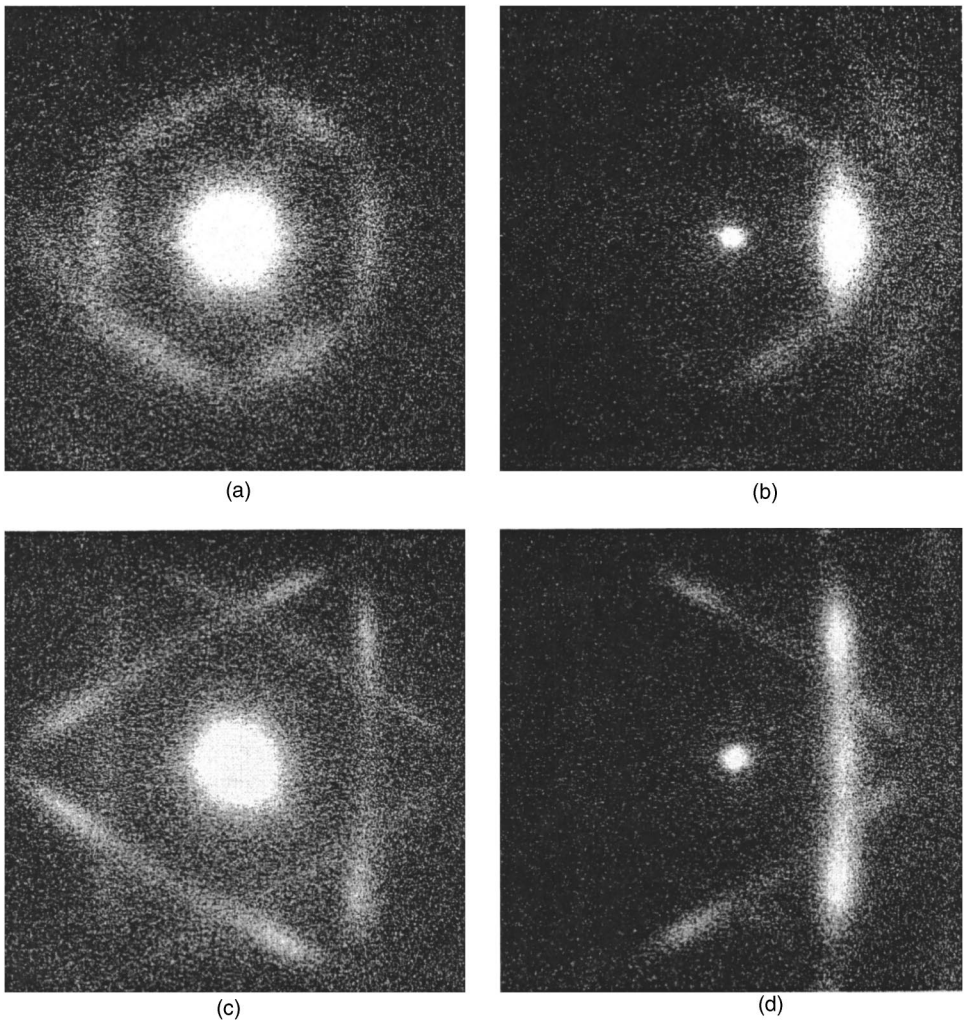

FIG. 1. (a) Diffraction pattern (for 1.4 ML on the α-$\sqrt{3}\times\sqrt{3}$ at 180 K) close to the (00) spot showing the "hexagonal" ring at 10.9%BZ along $[1\bar{1}0]$. (b) The pattern close to the Si(10) spot showing a broad Pb(10) spot with maximum intensity along $[1\bar{1}0]$. For (c) and (d) an additional 1.9 ML have been deposited. (c) The evolution of pattern (a) to a "starlike" pattern and (d) the evolution of (b) towards islands misoriented by 5.6° from $[1\bar{1}0]$.

iting 1.4 ML of Pb on the α-$\sqrt{3}\times\sqrt{3}$ at 180 K (the α-$\sqrt{3}\times\sqrt{3}$ phase requires $\sim 4/3$ ML). For this coverage 2-step islands are present as seen from the 2-layer oscillation of the intensity vs electron energy curve (not shown). A "hexagonal" pattern is visible around the (00) and Si(10) spots. In addition a bright Pb(10) is observed to the right of the Si(10) spot with its maximum intensity on the $[1\bar{1}0]$ azimuth, which shows that the islands are aligned with the [11_0] substrate direction. The position of the "hexagon" is 10.9%BZ of the Si(111) Brillouin zone (BZ) which agrees with the corrugation period 3.5 nm. The "hexagonal" shape observed in reciprocal space corresponds to the shape of the overlapping region formed by overlaying the Si(111) and Pb(111) lattices. Figure 1(c) shows the pattern change when 1.9 ML is added on top of the amount of Fig. 1(a). As seen in diffracted intensity vs electron energy measurements the islands still have the same 2-step height but they have grown laterally. The "hexagon" around the (00) spot changes to "starlike" pattern, while at the same time the orientation of the islands, as seen in Fig. 1(d), changes with the lobes of maximum intensity 5.6° rotated from the $[1\bar{1}0]$ direction. The relative rotation of the lattices causes changes in the shape of the overlapping region in real space which causes intensity redistribution in reciprocal space generating the starlike feature. This angle is larger than 3° observed for islands grown on top of the β-$\sqrt{3}\times\sqrt{3}$ (which has coverage 1/3 ML) or on the "SIC" (striped incommensurate) phase because a very smooth "devil's staircase" phase is present.[18]

An estimate of the amplitude of the atom relaxation at the interface can be made from the intensity ratio $\sim 1/100$ of the "hexagon" intensity to the intensity of the (00) spot. If a simple 1D model is used with the substrate modeled as a periodic lattice of coincidence cells of period $9a_0$ at position $r_j = j(9a_0)$ with j an integer, the intensity can be expressed as the product of the intensity due to the long range order times the scattering factor of the coincidence cell $I = |\Sigma_{j=1} \exp(ik_{\parallel} r_j)|^2 x |\Sigma_{n=1}^{n=10} \exp(ik_z \Delta z_n)|^2$ (with Δz the average atom shift, $k_{\parallel} = \pi a_0/9$ for the hexagon intensity and $k_{\parallel} = 0$ for the specular beam) then the measured intensity ratio 1/100 at 38 eV implies that $\Delta z \approx 0.048$ nm (i.e., for simplicity of the calculation we have assumed a "square-wave" displacement with half of the Pb atoms within the $9a_0$ coincidence cell displaced up and the other half down by Δz).

Since the 10.9%BZ diffraction feature of the pattern corresponds to the corrugation period and since the elastically scattered LEED electrons are unrelated to the QSE electrons, this provides solid confirmation that the geometric relaxation is the predominant contribution to the corrugation. Furthermore the intensity of the "hexagon" vs energy follows a

U-shaped curve, it is higher at lower energy used (~38 eV), then it decreases with increasing energy but at ~140 eV, it grows back again. Although the measurement is carried out on an island of finite thickness, this dependence is similar to the variation of the electron mean free path Λ with energy on macroscopic crystals[19] which also shows energy minimum at ~100 eV. This is consistent with the minimum electron penetration Λ within the island [and therefore reduced intensity of the incident electron beam at the interface as expected from its exponential dependence on $zI = I_0 \exp(-z/\Lambda)$].

In a theoretical study,[12] it was concluded that the Pb islands must be relaxed by comparing measured and calculated topography STM images. If the islands were not relaxed then there would be a dependence of the corrugation contrast on tunneling voltage while experimentally no contrast reversal is seen, i.e., the compact regions are always the bright ones. These regions correspond to Pb atoms adsorbed at T1 sites. The observed corrugation amplitude in STM is 0.06 nm consistent with the relaxations deduced in the calculation, i.e., the layer closer to the substrate has shift 0.052 nm, the middle layer has shift 0.062 nm and the top layer has shift 0.042 nm. These values agree well with the value of Δz from diffraction.

This conclusion is further confirmed with STS experiments in the range −1.5 V to 1.5 V shown in Fig. 2. An amount of 5 ML of Pb was deposited on an α-$\sqrt{3}\times\sqrt{3}$ substrate at 180 K and with the application of a high voltage pulse (~10 V) a nonequilibrium island height distribution was generated.[16] The area shown is 69×70 nm^2 and includes three different heights (marked in the image as 4-, 5-, 6-layer) islands separated by the α-$\sqrt{3}\times\sqrt{3}$ marked as the wetting layer (W.L.). The island height is measured from the W.L. so it is one layer less than heights measured from the Si substrate. The reference parameters are $V_{\mathrm{ref}} = 1$ V and $I_{\mathrm{ref}} = 0.5$ nA which correspond to a sample-tip separation approximately ≈ 0.8 nm.

First these spectroscopic data confirm the stability difference between even vs odd islands since the unstable heights (even) are of higher intensity than the stable height (odd). Their highest occupied band (HOB) is closer to the Fermi level.[16] The contribution of QSE is easily seen by naked eye for the stable 5-step island since at +0.45 eV the energy level of the lowest unoccupied band (LUB) as seen in the energy spectra,[16] the average current is higher. In addition, for this voltage the corrugation amplitude is enhanced, since as discussed before the optimal condition to observe the maximum corrugation is only 0.1 eV above the energy levels E_z.

It is also remarkable that the corrugation contrast in Fig. 2 does not change with tunneling voltage. This is seen in all STS images for 20 different tunneling voltages, but only six images are shown due to space limitations. At the bottom a region of the 0.45 eV image is shown at a much lower current level (reduced by a factor of ~10) to show that the contrast on the 5-layer island (which has low emission) is still unchanged. The contrast of the stable islands (5-layer) is complementary to the contrast of the unstable islands (4-, 6-layer) with their compact regions always of lower intensity than the surrounding "sea." The independence of the contrast in STS images confirms again that QSE cannot be the only mechanism responsible for the corrugation.

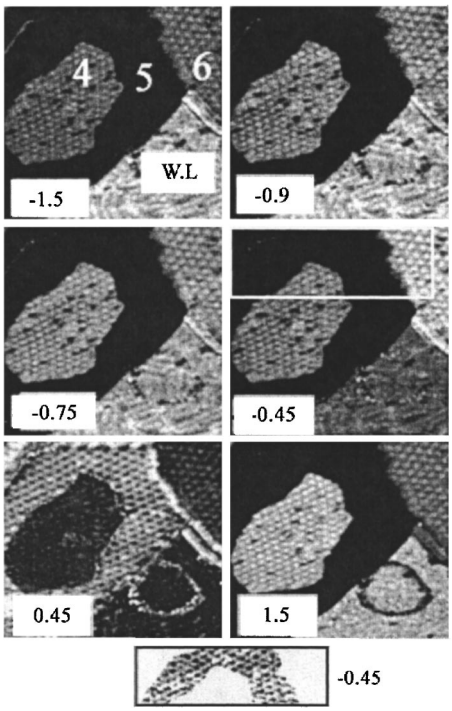

FIG. 2. STS images of size 69×70 nm^2 in the voltage range -1.5 V $< V <$ 1.5 V for 5 ML Pb grown on α-$\sqrt{3}\times\sqrt{3}$ at 180 K. Only images at 6 voltages are shown due to space limitations. Islands of unstable (4-, 6-layers) and stable (5-layer) heights are marked. The corrugation contrast is independent of the tunneling voltage. At the bottom a region of the image at 0.45 eV is shown at a much lower current level (reduced by a factor of ~10 from the full image) to show that the contrast on the 5-layer island (which has low emission) is still unchanged.

The results shown in Fig. 2 are standard STS images constructed from I–V curves obtained at each (x,y) lateral location and at constant tip-surface separation. The brightest region corresponds to the maximum current and the darkest to the minimum current for each image. Since the main conclusion depends on the sign of the contrast (i.e., bright regions remain bright and dark remain dark with tunneling voltage) and not on its absolute value, this presentation illustrates best the conclusion.

Figure 3 shows a calculation of STS image for a 2-step island [i.e., 3-step island if measured from the Si(111) substrate as in Ref. 12, for different tunneling voltages. Details of the calculation based on tight binding interaction potential can be found in Ref. 12]. For calculating the STS images we denote the variation of the STM tip height $\Delta z_V(x,y) = z_V(x,y) - \overline{z}$ at the scanned voltage V and $\Delta z_{\mathrm{ref}} = \Delta z_{\mathrm{ref}}(x,y) = z_{\mathrm{ref}}(x,y) - \overline{z}$ at the reference voltage V_{ref} defined by contours of constant local density of states (and therefore constant tunneling current) at average $\overline{z} = 0.8$ nm. This is based on the standard approximation[12] that the local density of states is proportional to the measured tunneling current I_m. If the tip-surface separation is kept constant as in STS (instead of the tunneling current) I_m can be written to first order as

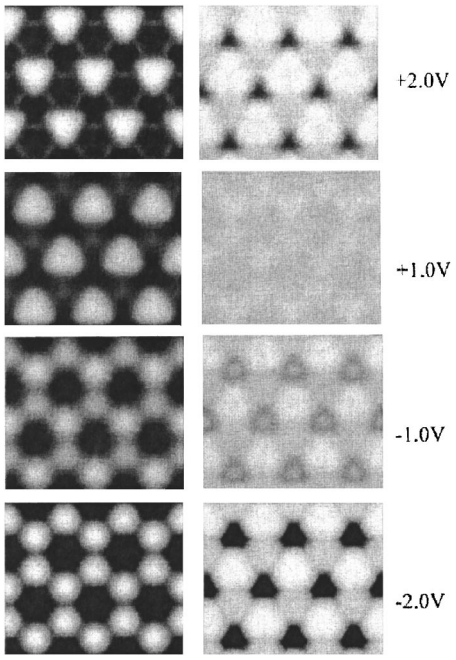

FIG. 3. Calculated STS images for a 2-step Pb island [i.e., 3-step when measured from Si(111)] on α-$\sqrt{3}\times\sqrt{3}$ as a function of tunneling voltage for unrelaxed islands (left column) and relaxed islands (right column). No change of contrast is seen for relaxed islands as in the experiment.

$$I_m \sim \overline{I} + \frac{dI}{dz}(\Delta z_V - \Delta z_{\mathrm{ref}}),$$

where $\overline{I}$ is the average tunneling current for V and dI/dz is the local "work function" evaluated at $\overline{z}$ and V. This is the current measured at constant tip surface separation as in the experiment. This expression can be rewritten in terms of calculated quantities in constant height images,

$$I_m \sim \overline{I} + \frac{dI}{dz}\left(\frac{\Delta I}{\left(\frac{dI}{dz}\right)} - \frac{\Delta I_{\mathrm{ref}}}{\left(\frac{dI_{\mathrm{ref}}}{dz}\right)}\right),$$

where $\Delta I = I - \overline{I}$ and $\Delta I_{\mathrm{ref}} = I_{\mathrm{ref}} - \overline{I}_{\mathrm{ref}}$ are the variations in the tunneling current at the lateral location (x,y) for V and V_{ref}, respectively and dI_{ref}/dz is the local work function at $\overline{z}$ and V_{ref}.

The results of the calculation are shown in Fig. 3 for four scanned voltages of positive and negative polarity. The shown intensity is proportional to the density of states and, since the conclusion is based only in the absence of contrast variation as the tunneling voltage is changed, the absolute intensity level is unimportant. If the island is not relaxed then there is a dependence on voltage contrary to the experiment, while for relaxed islands this is not the case.

In summary, we have presented complementary STM, STS, and SPA-LEED experiments studying the corrugation observed on top of Pb islands grown on the α-$\sqrt{3}\times\sqrt{3}$ phase. Calculated STS and topography images were used to deduce that the observed independence of the corrugation contrast on tunneling voltage can only be explained from the geometric relaxation in the islands. This is further supported from the SPA-LEED experiments which are only sensitive to the atom relaxation. Such studies offer a different possibility to probe metal/semiconductor interfaces.

Ames Laboratory is operated by the U.S. Department of Energy by Iowa State University under Contract No. W-7405-Eng-82. This work was supported by the Director for Energy Research Office of Basic Energy Sciences.

*Electronic address: tringides@ameslab.gov; Fax: 515 294 0689.

[1] M. Jalochowski, H. Knoppe, G. Lilienkamp, and E. Bauer, Phys. Rev. **46**, 4693 (1992).
[2] B. J. Hinch, C. Koziol, J. P. Toennies, and G. Zhang, Europhys. Lett. **10**, 341 (1989).
[3] T. C. Chiang, Surf. Sci. Rep. **39**, 181 (2000).
[4] I. B. Altfeder, K. A. Matveev, and D. M. Chen, Phys. Rev. Lett. **78**, 2815 (1997).
[5] K. Budde, E. Abram, V. Yeh, and M. C. Tringides, Phys. Rev. B **61**, 10 602 (2000).
[6] A. R. Smith, K. J. Chao, Q. Niu, and C. K. Shih, Science **273**, 226 (1996).
[7] Z. Zhang, Q. Niu, and C. K. Shih, Phys. Rev. Lett. **80**, 5381 (1998).
[8] C. M. Wei and M. Y. Chou, Phys. Rev. B **66**, 233408 (2002).
[9] E. Ogando, N. Zabala, E. V. Chulkov, and M. J. Puska, Phys. Rev. B **69**, 153410 (2004).
[10] V. Yeh, L. Berbil-Bautista, C. Z. Wang, K. M. Ho, and M. C. Tringides, Phys. Rev. Lett. **85**, 5158 (2000).
[11] W. B. Jian, W. B. Su, C. S. Chang, and T. T. Tsong, Phys. Rev. Lett. **90**, 196603 (2003).
[12] T. L. Chan, C. Z. Wang, M. C. Tringides, W. C. Lu, and K. M. Ho, Phys. Rev. Lett. (unpublished).
[13] K. A. Edwards, P. B. Howes, J. E. Macdonald, T. Hibma, T. Bootsma, and M. A. James, Surf. Sci. **424**, 169 (1999).
[14] H. H. Weitering, D. R. Heslinga, and T. Hibma, Phys. Rev. B **45**, 5991 (1992).
[15] R. Zdyb and E. Bauer, Phys. Rev. Lett. **88**, 166403 (2002).
[16] M. Hupalo and M. C. Tringides, Phys. Rev. B **65**, 115406 (2002).
[17] K. Kobayashi, Phys. Rev. B **53**, 11 091 (1996).
[18] M. Hupalo, J. Schmalian, and M. C. Tringides, Phys. Rev. Lett. **90**, 216106 (2003).
[19] M. G. Lagally, in *Methods of Experimental Physics Solid State Physics Surfaces*, edited by R. L. Park and M. G. Lagally (Academic, New York, 1985), Vol. 22.